

# Observations of sediment transport during the inundation of a barrier island

Anita Engelstad<sup>1</sup>, Maarten van der Vegt<sup>1</sup>, Gerben Ruessink<sup>1</sup>, and Piet Hoekstra<sup>1</sup>  
<sup>1</sup> Utrecht University, The Netherlands  
 email: [A.C.Engelstad@UU.nl](mailto:A.C.Engelstad@UU.nl)



Utrecht University

## Introduction

Overwash and inundation transport sediment onshore. This onshore transport can potentially ensure the aggradation of barrier islands, particularly along the Dutch coast. To allow for vertical growth of these barrier island in times of sea-level rise, the re-opening of dunes and dykes in uninhabited areas in the Netherlands is considered. But first it is necessary to gain more insight into the processes that govern sand transport during inundation.

## Research Questions

- What is the magnitude and direction of sand transport during inundation?
- What is the relative importance of waves and currents for sand suspension and transport processes?
- How do transport processes vary over time and between inundation events?

## Field site



Figure 1. The barrier island of Schiermonnikoog is located in the North Sea and is separated from the Dutch coast by the Wadden Sea. The field site was located on the eastern tip of the island.

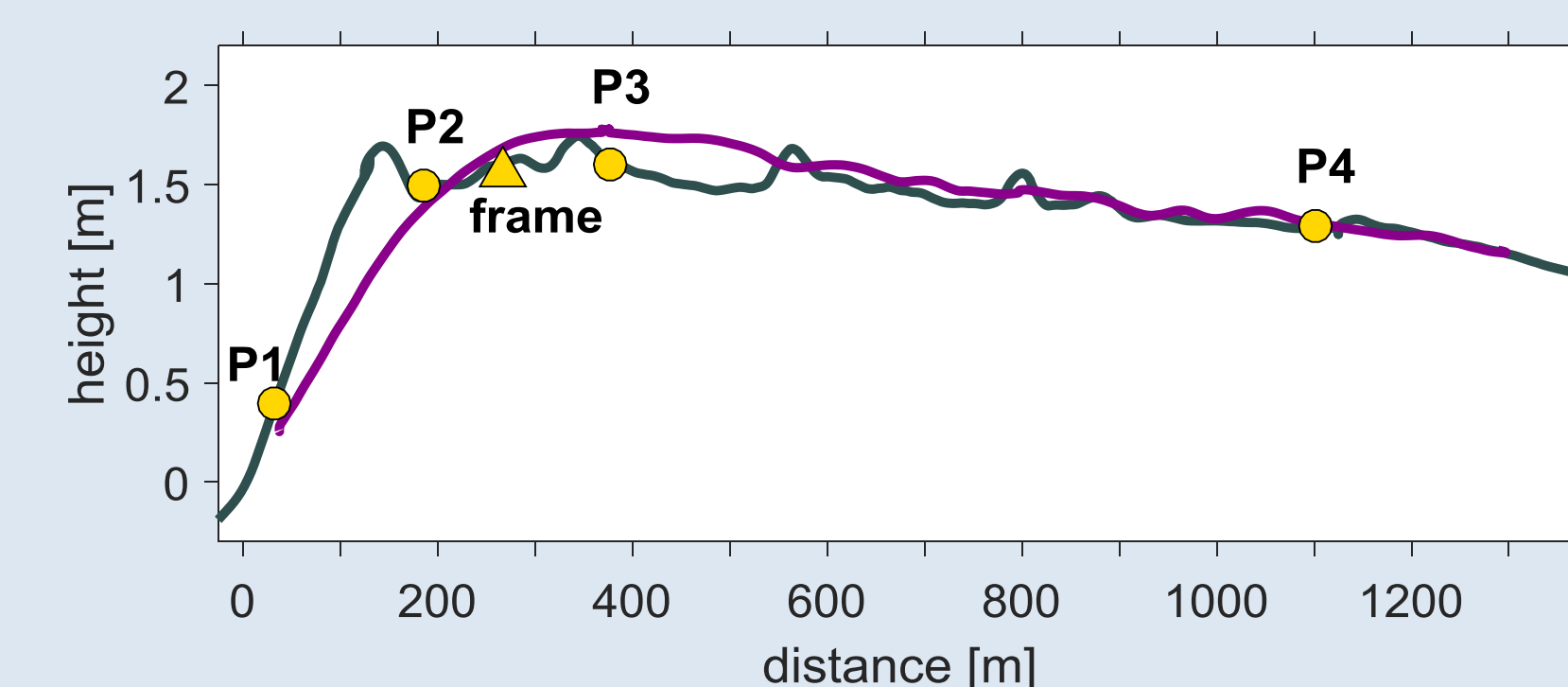


Figure 2. Initial (grey line) and final (magenta line) cross-island profiles with the North Sea to the left and the back barrier area (Wadden Sea) to the right. Yellow dots indicate the locations of stand-alone pressure sensors, the yellow triangle shows the location of the instrument frame.

## Methods

### Instrumentation

4 stand-alone pressure sensors measured at 10 Hz continuously, while 1 ADVO (pressure and currents) and 5 STMs (suspended sediment concentrations), mounted on a frame (Figure 2), measured at 4 Hz during inundations only.

### Data analysis

Bulk data is averaged over 15 minutes. Velocities were bandpass filtered to estimate infragravity (0.005-0.05 Hz) and short wave (0.05-1 Hz) velocities. STM availability varied due to burial and un-burial of sensors. To account for variations in sensor height, sand concentrations were linearly fitted to yield concentrations  $C_{fit}$  at height  $z$  and depth-integrated:

$$c(t) = \int_0^d C_{fit}(t, z) dz$$

where  $d$  is the water depth. The net total depth-integrated transport  $\vec{Q}$  was calculated as:

$$\vec{Q} = \frac{1}{T} \int_0^T \int_0^d \vec{U}(t, z) C_{fit}(t, z) dz dt$$

$\vec{U}$  is the velocity vector at height  $z$ , estimated by a log-profile (Karman-Prandtl boundary equation) from the single point measurement. The forcing is estimated by the Shields parameter  $\theta$  and is calculated as

$$\theta = \frac{\tau}{\rho_s - \rho_w g d_{50}}$$

$\tau$  is the bed shear stress forced by the cross- and alongshore flow,  $\rho_w$  is the density of water and  $\rho_s$  is the density of sand,  $g$  is the gravitational acceleration and  $d_{50}$  is the median grain size (203  $\mu\text{m}$ ). We present here 3 out of 7 recorded floodings, chosen for their different hydrodynamic conditions

## Results

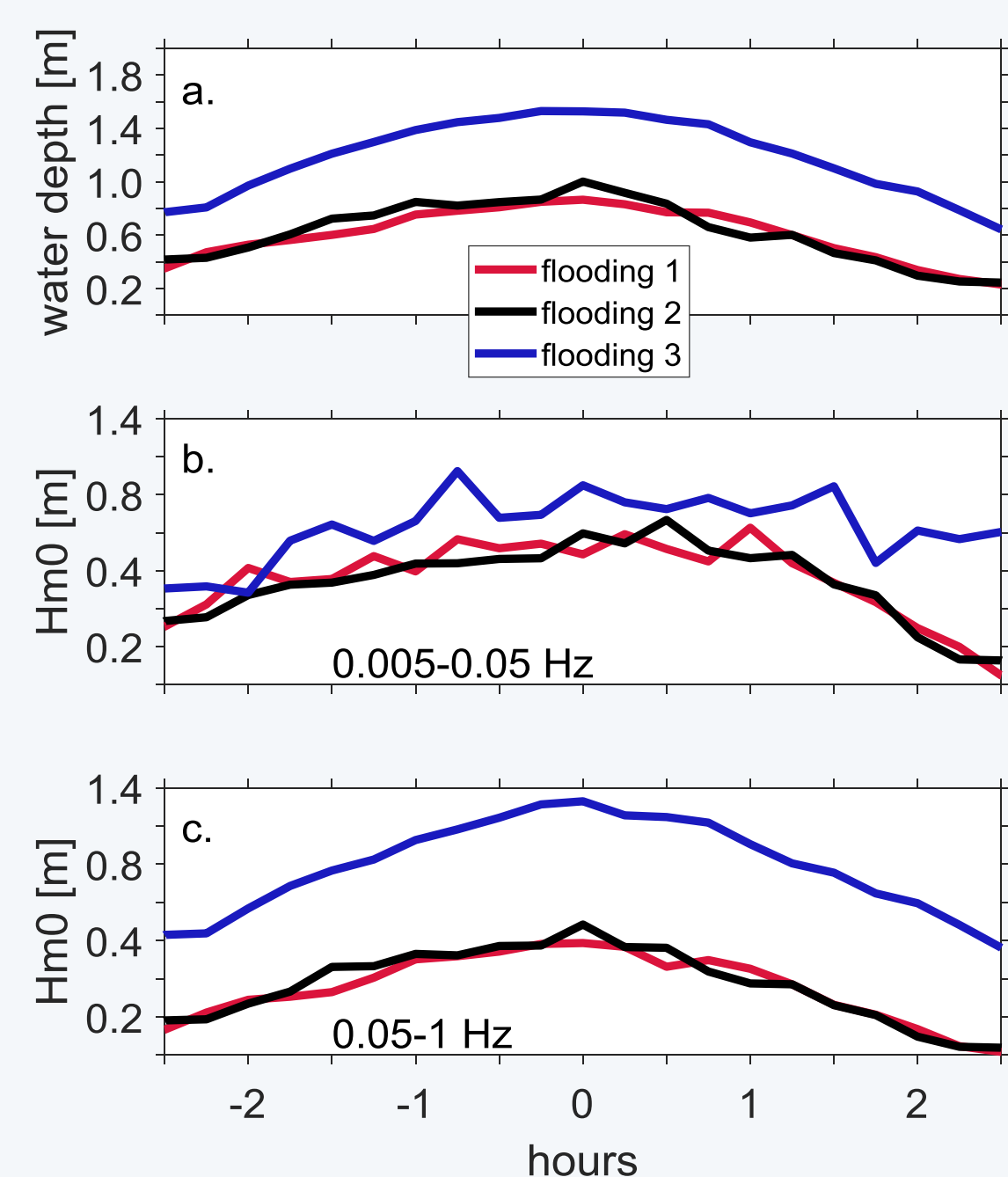


Figure 3. Inundation depths (a.), infragravity (b.) and short (c.) wave heights at P2 for 3 different floodings. The x-axis shows the time relative to high tide (0 hours).

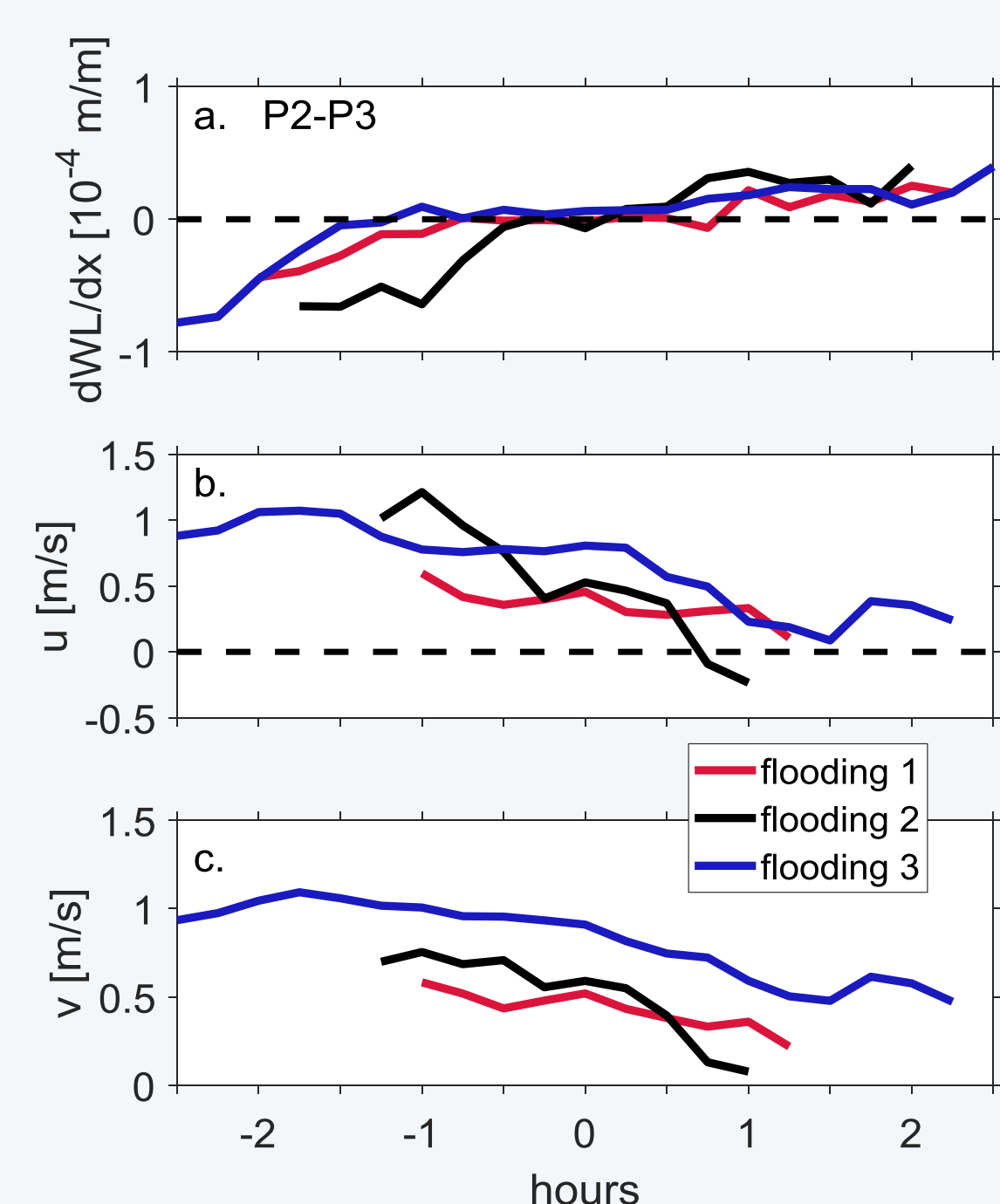


Figure 4. Water level gradients (a.), depth-averaged cross-shore (b.) and alongshore (c.) velocities at the frame. Negative  $dWL/dx$  and positive  $u$  are landwards, while positive  $v$  is approximately towards the East. The x-axis shows the time relative to high tide (0 hours).

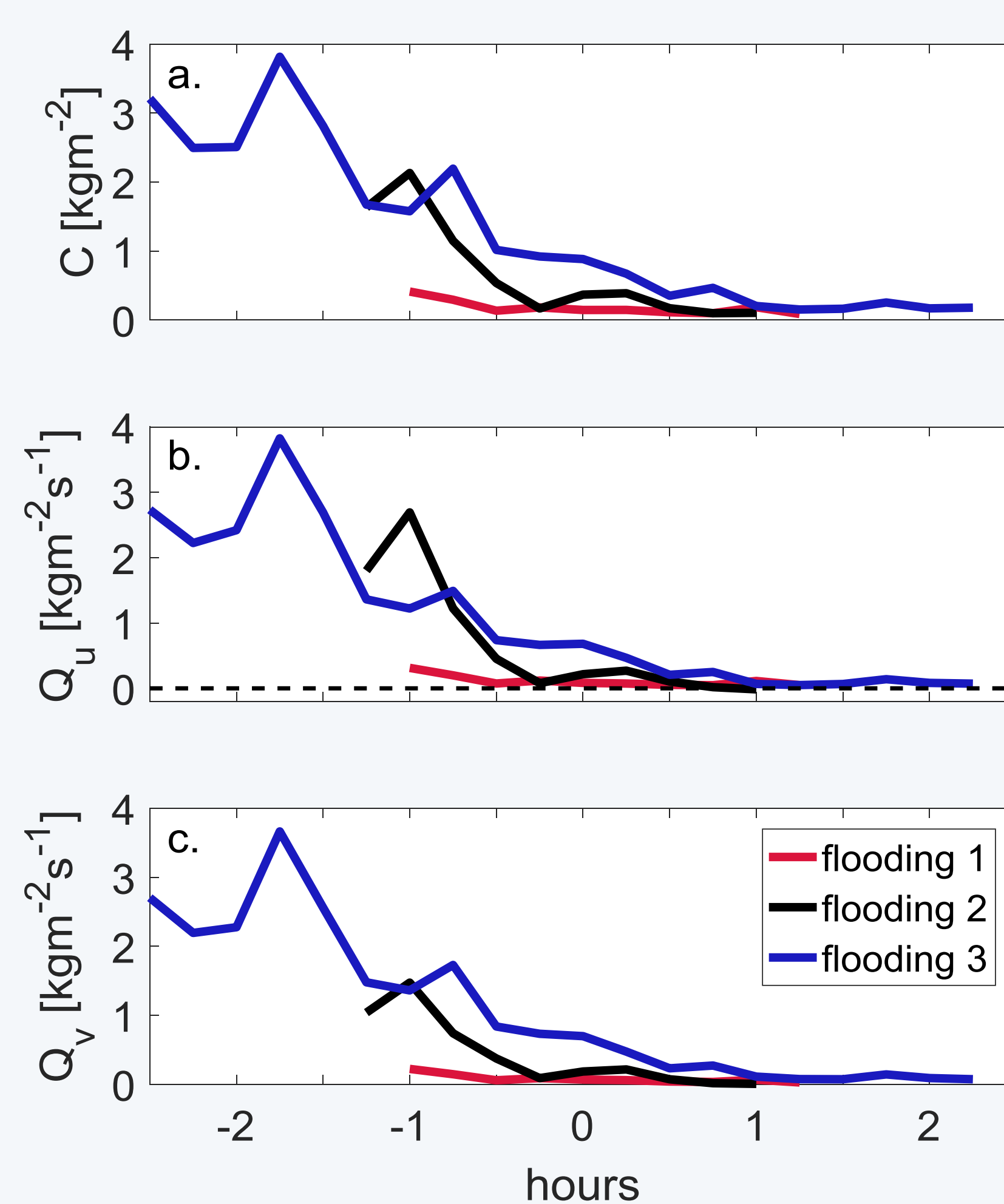


Figure 5. Net depth-integrated suspended sediment concentrations, (a.), cross-shore (b.) and alongshore (c.) sand transport. Positive  $Q_u$  is landwards, while positive  $Q_v$  is approximately towards the East. The x-axis shows the time relative to high tide (0 hours).

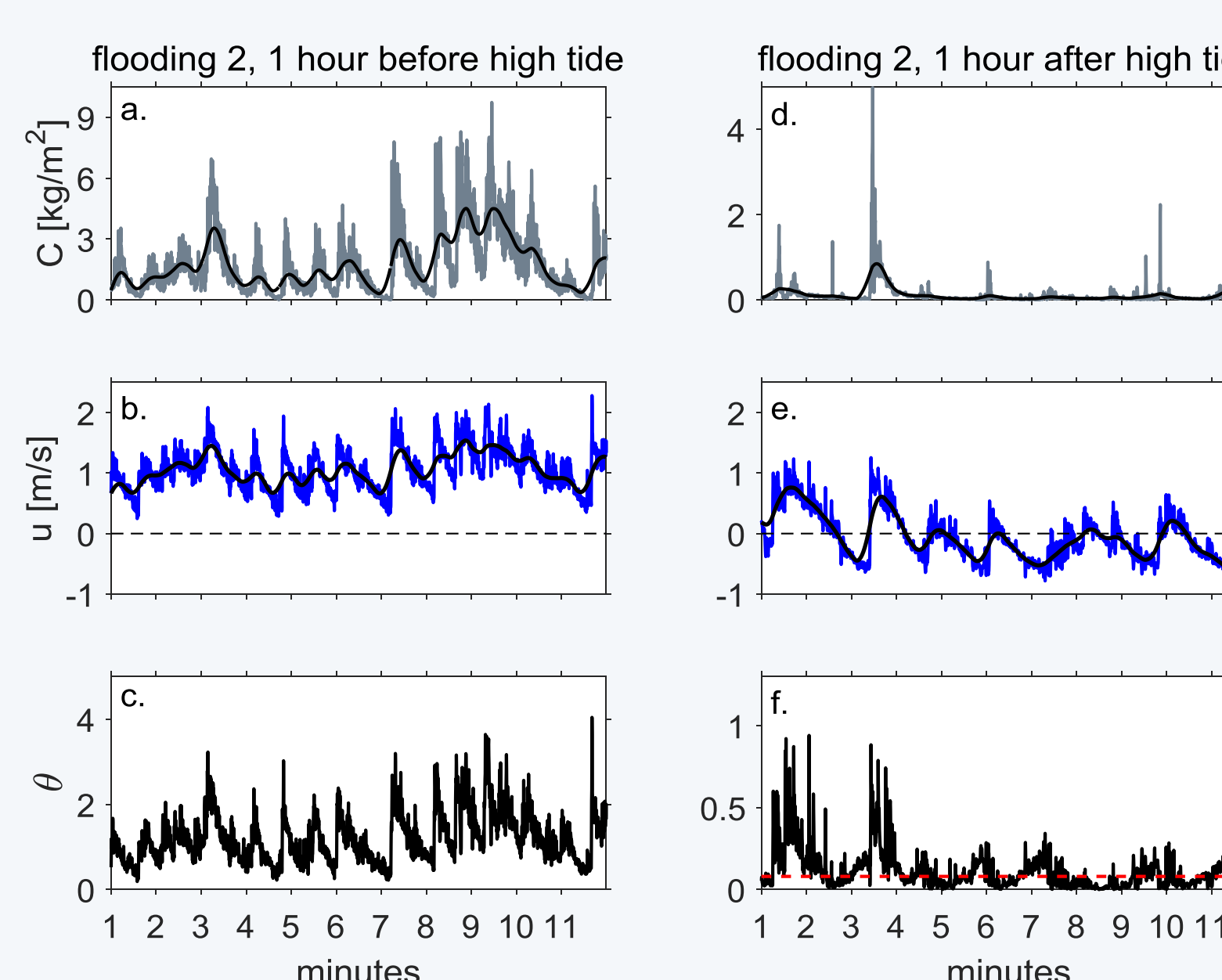


Figure 6. Instantaneous depth-integrated suspended sediment concentrations (a and d), measured at the lowest STM, compared to depth-averaged cross-shore velocities (b and e) and Shields parameters (c and f) for flooding 2. The red dashed line in (f) shows the critical Shields parameter for suspension. Note the different vertical scales.

### Acknowledgements

We are grateful for the technical support of Marcel van Maarseveen, Henk Markies, and Arjan van Eijk. We would also like to thank Daan Wesselman and Natuurmonumenten for their assistance during the field work. This work is supported by NWO.

## Main Findings

- Sand suspension and transport were usually highest at the onset of inundations, dependent on the magnitude of the mean current velocities. Cross-shore velocities were affected by the water levels in the Wadden Sea (Figure 4).
- Sand transport was directed almost entirely onshore and towards the East. Offshore transport was negligible (Figure 5).
- High concentrations of suspended sediment were mainly forced by the combined bed shear stresses of infragravity waves and currents (Figure 6).
- The dominant cross-shore sand transport mechanism was the mean cross-shore current. Short wave transport was negligible, while infragravity wave transport became important when mean currents were  $\sim < 0.5$  m/s (Figure 7).
- Even though water levels and waves were similar during floodings 1 and 2, cross-shore currents and therefore the net depth-averaged sand transport was higher during flooding 2 ( $\sim 5660 \text{ m}^3/(\text{m width})$ ) compared to flooding 1 ( $\sim 1049 \text{ m}^3/(\text{m width})$ ) due to the stronger water level gradient. During flooding 3  $\sim 11190 \text{ m}^3/(\text{m width})$  of sand were transported landwards.

## Discussion

Onshore directed current velocities in our field area were generally strong but greatly reduced after high tide, because water levels in the Wadden Sea were elevated. Since sand transport is dominated by the mean currents, this suggests that the processes in the Wadden Sea reduce the accretion of sediment on the island.